Kidney International, Vol. 41 (1992), pp. 1366–1373

A model of the volumetrically-controlled hemodialysis circuit

THOMAS L. PALLONE, SCOTT W. HYVER, and JEFFREY PETERSEN

Divisions of Nephrology, Stanford University Hospital and Palo Alto Veterans Administration Medical Center, Palo Alto, California, and the Pennsylvania State University, Hershey, Pennsylvania, USA

A model of the volumetrically-controlled hemodialysis circuit. We developed a model that predicts the hemodynamics of the volumetrically-controlled circuit used to administer high flux hemodialysis. The equations simulate the entire blood side of the circuit so that blood and dialysate pressures can be predicted from a knowledge of circuit component and patient characteristics. An alternative method of computation has also been devised which permits measured circuit pressures to be used to predict patient blood access pressure, dialyzer resistance to flow and membrane hydraulic conductivity. Success of the model was evaluated by measuring both circuit pressure and component characteristics. The model successfully predicted circuit pressures when measured component characteristics were employed as model inputs. Conversely, the model accurately predicted circuit component characteristics when measured pressures were employed as inputs (8 patients, 30 dialyses). Specific predictions of the model include the following. Elevations of patient blood access pressure will cause blood and dialysate pressures to rise equivalently without affecting the rate of backfiltration or location of pressure equilibrium along the dialyzer axis. Elevated hematocrit is predicted to increase circuit pressures to a degree that is similar to a poorly functioning blood access, however, high hematocrit markedly augments backfiltration and moves the point of pressure equilibrium toward the dialyzer entrance. We conclude that the model provides a predictive tool that can be used to optimize circuit design. Alternatively, the model can be used to separate the influence of a poorly functioning patient access from other factors which can elevate circuit pressures.

The availability of synthetic membranes with high hydraulic water and solute permeabilities has facilitated the emergence of high flux hemodialysis. With this modality, it is often the patient rather than the dialysis system that limits the rate of mass transfer that can be delivered [1]. For dialysis time to be shortened, the patient must have an adequate blood access to achieve the desired blood flow and must tolerate rapid volume and solute removal without concomitant hypotension or disequilibrium.

In order to limit ultrafiltration, volumetrically-controlled dialysate delivery systems have been designed. Generally, a positive dialysate pressure is maintained to limit the transmembrane pressure gradient to that required to facilitate ultrafiltration. Recently, we have shown that a straightforward hemodynamic description of the extracorporeal circuit suffices to simulate many aspects of slow continuous renal replacement therapies [2, 3]. To enable prediction of blood and dialysate side pressures during high flux hemodialysis we have extended those models to the hemodialysis circuit. To verify the predictive capacity of the model, measurements taken during dialysis runs were compared with predictions.

Received for publication July 22, 1991
and in revised form December 3, 1991
Accepted for publication December 5, 1991

Methods

Patient measurements

Measurement of blood and dialysate inlet and outlet pressures were performed during high flux dialysis treatments using the Fresenius F80 dialyzer (Fresenius Inc., Concord, California, USA). Plasma protein concentrations were measured by the method of Lowry, Rosenbrough and Farr [4] and hematocrits by centrifugation. Thirty dialyses were studied in eight patients at filtration rates of 0.5 to 2.5 liters/hr. All dialyses were performed with the same type of arterial and venous tubing and access needles. Mean values for patient hematocrit, plasma protein concentration, blood and dialysate inlet and outlet pressures are shown in Table 1. Intrapatient data variation was much smaller than interpatient variation. Consistent with this, the entries in Table 1 and Table 4 were obtained by taking the averages for individual patients and placing the mean ± SD of those eight averages in the tables.

Component resistance and hydraulic conductivity

As previously described, the resistance to flow of the blood side of the dialyzer, venous tubing and access needle were measured by perfusing these components with 40% sucrose at known pressures. Perfusion with 40% sucrose enabled measurements to be obtained during laminar flow. The pressure-to-flow rate ratio was divided by the viscosity of sucrose at 23°C (7.01×10^{-7} mm Hg · min) to yield the resistance [2]. Since flow on the dialysate side of the membrane is probably turbulent, measurements of dialysate side resistance to flow were not obtained by this method. Measurements of the pressure drop across the dialysate path obtained during patient dialyses sufficed to define this effect because inlet dialysate flow was always 800 ml/min.

Dialyzer hydraulic conductivity was measured by the method previously described [2, 3] assuming a surface area of 1.8 m^2. In view of the marked change in hydraulic permeability (L_p) of polysulfone membranes induced by contact with plasma proteins [2], these measurements were repeated before and after exposure to patient blood.

Experimental results are expressed as mean ± SD

Table 1. Patient characteristics

N	H	C_{pi}	P_{bi}	P_{bo}	P_{di}	P_{do}
30	0.32 ± 0.09	7.0 ± 0.7	252 ± 76	157 ± 40	164 ± 48	99 ± 54

Table entries expressed as mean ± SD.

Mathematical model

Pressure distribution. In the conventional or high-flux hemodialysis circuit blood is pumped from the patient at a preset flow rate into the entrance port of a dialyzer. This process raises the pressure at the dialyzer inlet (P_{bi}) to the level needed to drive flow through the downstream series of resistances (R) represented by the dialyzer (R_b), venous tubing (R_{vt}) and venous needle (R_{vn}). In order to simulate the blood side pressure (P_b) along the dialyzer axis, we employ the differential form of Poiseuille's equation [2],

$$\frac{d}{dx}(P_b) = -\frac{R_b}{L}\mu_b Q_b \tag{1}$$

where L is the dialyzer length, μ_b is blood viscosity and Q_b is blood flow rate. For a hollow fiber dialyzer, R_b can be computed from the fiber number (N), internal radius (r) and length (L) as

$$R_b = \frac{8L}{N\Pi r^4} \tag{2}$$

Upon exiting the dialyzer, P_b will continue to decrease, eventually reaching the exit pressure of the circuit (P_v) at the end of the venous needle within the patient's arm.

$$P_v = P_{bo} - (R_v)\mu_b Q_{bo} \tag{3}$$

where P_{bo} and Q_{bo} are blood side pressure and flow rate at the dialyzer outlet and $R_v = R_{vt} + R_{vn}$. On the dialysate side, we compute dialysate pressure (P_d) in a similar manner.

$$\frac{d}{dx}(P_d) = +\frac{R_d}{L}\mu_w Q_d \tag{4}$$

where μ_w is dialysate viscosity (equal to that of water). A simple relationship like equation 2 is not available to compute R_d. Indeed, flow on the dialysate side is likely to be turbulent so that a linear relationship between pressure and flow undoubtedly represents an oversimplification [5, 6]. Since the rate at which filtrate is added to dialysate from the blood is small compared to the rate of dialysate flow at dialyzer inlet (Q_{di}), equation 4 is tantamount to assuming a linear pressure profile along the dialyzer axis.

Conservation equations. Blood flow in the dialyzer is equal to the sum of plasma (Q_p) and RBC flow (Q_c). The latter is expected to be constant ($Q_c = H\ Q_{bi}$) while plasma flow rate varies with position (x) along the dialyzer axis. Conservation of volume requires

$$\frac{d}{dx}(Q_p) = -J_v\frac{S}{L} \tag{5}$$

and

$$\frac{d}{dx}(Q_d) = -J_v\frac{S}{L} \tag{6}$$

where J_v is the rate of transmembrane volume flux and S is the total surface area for filtration. J_v is defined by [7]

$$J_v = L_p\{(P_b - P_d) - \Pi_p\} \tag{7}$$

where L_p is hydraulic conductivity and Π_p is plasma oncotic pressure [8].

$$\Pi_p = 2.1C_p + 0.16C_p^2 + 0.009C_p^3 \tag{8}$$

C_p is plasma protein concentration which can be computed from its systemic value at the dialyzer entrance (C_{pi}) according to

$$C_p = C_{pi}\frac{Q_{pi}}{Q_p} \tag{9}$$

Equations 7 to 9 assume that a radial concentration gradient is not established across the hollow fiber due to the rejection of proteins at the membrane surface. The validity of this is reviewed in this document at a later point.

Blood rheology. Blood viscosity (μ_b) varies as a function of plasma protein concentration and the changing hematocrit (ϕ) along the axis of the dialyzer. To enable computation of μ_b, we employ the method previously described [3]. These relationships, reproduced below, are based on the work of Merrill [9, 10] and Vand [11], and do not account for partitioning of RBCs and plasma at the dialyzer entrance. Accordingly, alteration of hollow fiber hematocrit and viscosity due to the Fahraeus [12] and Fahraeus-Lindqvist [13] effects are neglected. The data supporting this description of the rheological properties of blood, and the consequent limitations imposed upon extrapolation of the model have been discussed in detail [2, 3].

$$\mu_{b,37} = \mu_{p,37}(1 + 2.5\phi + 0.0735\phi^2) \tag{10}$$

where $\mu_{b,37}$ and $\mu_{p,37}$ are blood and plasma viscosity at 37°C, respectively, and

$$\phi = \frac{Q_c}{Q_p + Q_c} \tag{11}$$

μ_p is computed from protein concentration [3],

$$\mu_{p,37} = \mu_{w,37} + (\mu_p' - \mu_{w,37})\frac{C_p}{C_p'} \tag{12}$$

where $\mu_{w,37}$ is the viscosity of water at 37°C, (0.864×10^{-7} mm Hg · min); μ_p' is normal plasma viscosity (1.54×10^{-7} mm Hg · min), at a plasma protein concentration C_p' of 7 g/dl [14].

Merrill et al demonstrated that μ_b varies with temperature in proportion to μ_w [10]. Thus,

$$\mu_b = \mu_{b,37}\left(\frac{\mu_{w,20}}{\mu_{w,37}}\right)\left(\frac{\mu_w}{\mu_{w,20}}\right) \tag{13}$$

where $\mu_{w,20}$ and μ_w are water viscosity at 20°C and temperature, T. The ratio of water viscosity at 20°C to that at 37°C is 1.449, and the ratio of water viscosity at any temperature, μ_w to that at 20°C is given by,

Table 2. Parameter inputs required for model simulations

Parameter	Chosen	Measured	Predicted
Q_b *ml/min*	450[a]		
Q_d *ml/min*	800[a]		
Q_f *ml/min*	33.3[a]		
H	0.30[a]		
C_p *g/dl*	7.0[a]		
T *°C*	37[a]		
S cm^2	18×10^3[a]		
L *cm*	22.5[a]		
N_f	13.5×10^3[a]		
r_f *cm*	0.01[a]		
P_v *mm Hg*			46[a]
R_b $\frac{1}{cm^3}$		4.85×10^5[a]	4.91×10^5
R_d $\frac{1}{cm^3}$			9.54×10^5[a]
R_v $\frac{1}{cm^3}$		5.88×10^5[a]	
L_p *cm/[min · mm Hg]*		6.91×10^{-5}[a]	6.24×10^{-5}

"Chosen" refers to values set to describe a typical high flux dialysis circuit or patient. "Predicted" values are obtained by running model in Mode 1 (see Table 3 and text).

[a] Used for "Base Case" model explorations

$$\frac{\mu_w}{\mu_{w,20}} = e^{\{2.303g(T)\}} \tag{14}$$

where g(T) is defined by,

$$g(T) = \frac{1.327(20 - T) - 0.00105(T - 20)^2}{T + 105} \tag{15}$$

Equations 14 and 15 are valid from 20°C to 100°C [15].

Computation, base case exploration. Differential equations were integrated on a Hewlett Packard RS/20 microcomputer using the method of Gear [16]. The parameters required to completely solve the model equations are listed in the left column of Table 2. Parameter values identified with an asterisk represent "base case" values used for model exploration in subsequent sections of this report. The base case values were "chosen" to typify the average characteristics of a patient undergoing high flux hemodialysis (Q_b, Q_d, Q_f, H, C_p, T), "measured" in vitro (R_b, R_v, L_p), or "predicted" by the model from patient data (P_v, R_d).

Computation requires the user to supply an initial guess for the dialysate outlet pressure (P_{do}) and blood inlet pressure (P_{bi}) at x/L = 0. The equations are solved to predict the circuit outlet pressure (P_v) and net filtration rate (Q_f). P_{bi} and P_{do} are iteratively adjusted until the predicted values of P_v and Q_f each agree with their input specification within a factor of 10^{-3}. The model yields predictions of the spatial variation of blood and dialysate hydraulic pressure, protein concentration, oncotic pressure, hematocrit, blood viscosity and transmembrane volume flux. The rates of forward and backfiltration are predicted as well as the point along the dialyzer axis where backfiltration begins.

Computation, model evaluation. To evaluate the model's success in predicting measured data from patient dialyses and in vitro measurements, the computer program that solves the system of equations was also written in one of two modes (Table 3). In Mode 1, Q_b, Q_d, Q_f, H, C_p, T, S, L, N_f, r_f and R_v for individual patient dialyses were supplied as inputs along with a guess of R_b, R_d, L_p and P_v. Pbi and Pdo measurements were supplied as inputs to the model to initiate integration at x/L = 0. The equations were integrated along the dialyzer from x/L = 0 to 1 to yield predictions of blood outlet (P_{bo}) and dialysate inlet (P_{di}) pressure, Q_f and P_v (equation 3). The parameters R_b, R_d, L_p were iteratively adjusted until predictions of P_{bo}, P_{di} and Q_f reproduced measurements for the individual dialysis run. Mode 1 was used to compare model predictions of R_b and L_p obtained by simulating patient data with measurements of R_b and L_p obtained in vitro. In Mode 2, R_b, R_d, L_p (mean in vitro measurements) and P_v (46 mm Hg) were supplied as inputs along with individual data (Q_b, Q_d, Q_f, H, C_p, T, S, L, N_f, r_f) for patient dialyses. P_{bi} and P_{do} at x/L = 0 were initially supplied as a guess and then iteratively adjusted until predicted Q_f and P_v agreed with input specifications. This yielded predictions of blood and dialysate pressures that could be compared with measurements obtained during patient dialyses. Mode 2 was used to compare model predictions of blood and dialysate pressures with in vivo measurements.

Table 3. Modes of computation

Parameter	Mode 1	Mode 2
P_{bi}	S	P
P_{bo}	S	P
P_{di}	S	P
P_{do}	S	P
R_b	P	S
R_d	P	S
L_p	P	S
P_v	P	S

Entries indicate whether the parameter was specified (S) as input or predicted (P) as a model output.

Table 4. Model predictions of target parameters

	$R_b \times 10^5$ $\frac{1}{cm^3}$	$R_d \times 10^5$ $\frac{1}{cm^3}$	$L_p \times 10^{-5}$ *cm/(min · mm Hg)*	P_v *mm Hg*
Mean ± SD	4.91 ± 0.81	9.54 ± 2.45	6.23 ± 1.37	46 ± 5.46
Meas (*N*)	4.85 ± 0.15(8)	—	6.91 ± 0.19 (7)	—
Calc	4.24			

Entries are the mean ± SD of parameter values either predicted by the model from patient simulations, or measured in vitro (Meas). (*N*) is the number of separate F80 dialyzers studied. The calculated value of R_b obtained from equation 2 is also given.

Results

Model predictions of target parameters

Thirty simulations of patient dialyses were performed in Mode 1 (Table 3). Individual patient values of Q_b, Q_d, Q_f, C_p, and H were supplied as inputs (Q_b was either 440 or 450 ml/min and Q_d was always 800 ml/min). Mean ± SD of the predictions of R_b, R_d, L_p and P_v for all patients are shown in Table 4. Measurements of R_b and L_p obtained in vitro are also provided for comparison.

For R_b, values predicted and measured were close and agreed satisfactorily with that calculated from Poiseuille's equation.

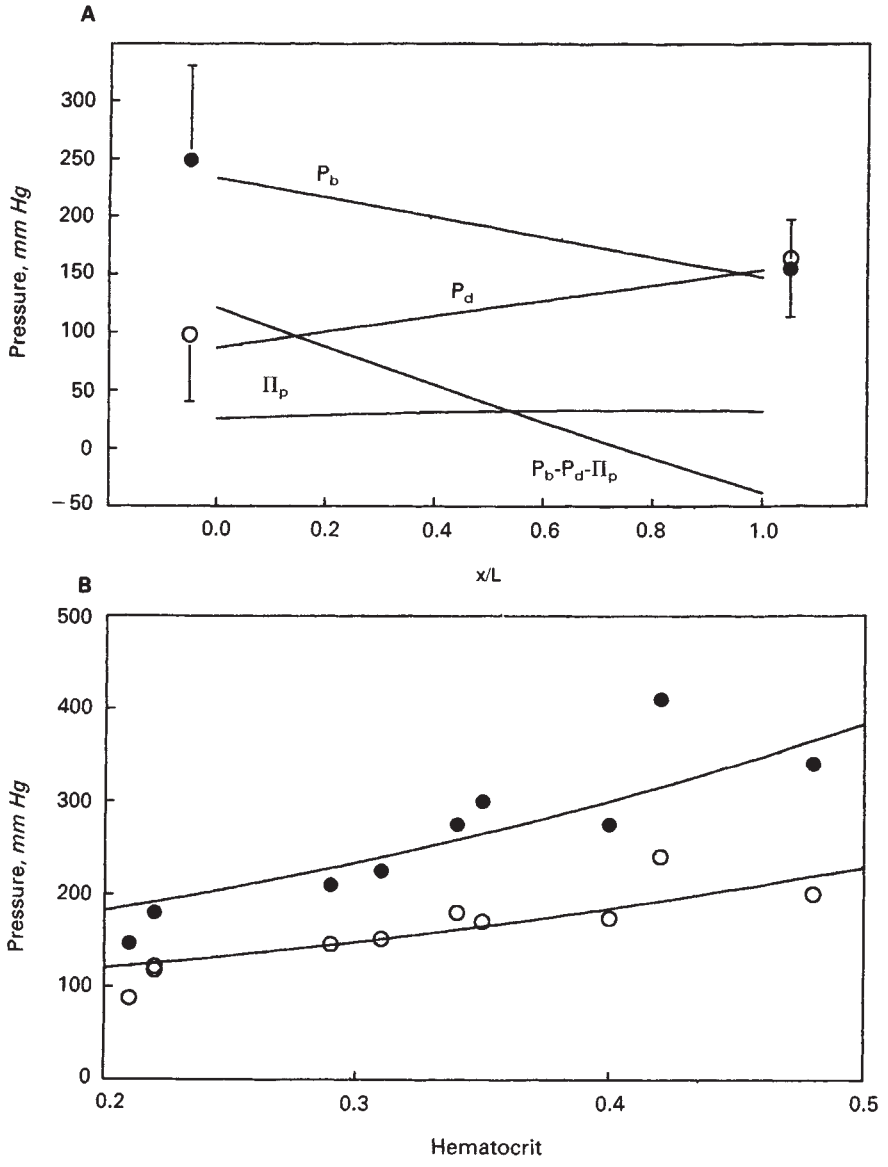

Fig. 1. *Comparison of model predictions with measurements.* **A.** Blood side (P_b) and dialysate side (P_d) pressures are shown as a function of location (x/L) along the dialyzer axis. Plasma oncotic pressure (Π_p) and the sum of these driving forces are given. Blood side (filled circles) and dialysate side (open circles) pressure measurements are also given at the blood inlet (x/L = 0) and outlet (x/L = 1) of the dialyzer. **B.** Measurements of blood inlet (filled circles) and outlet (open circles) pressures are shown as a function of systemic hematocrit. Solid lines are the base case model predictions.

Measurements of L_p obtained before and after exposure to blood revealed a decrease from $18.6 \times 10^{-5} \pm 0.65 \times 10^{-5}$ to $6.91 \times 10^{-5} \pm 0.19 \times 10^{-5}$ cm/(sec · mm Hg), respectively. The latter value of L_p is representative of in vivo conditions [2] and is in fair agreement with that predicted by Mode 1 simulations ($6.23 \times 10^{-5} \pm 1.37 \times 10^{-5}$, Table 4). It is interesting to note that P_v is predicted (46 ± 17, mean ± SD) to lie between the arterial and venous pressures of a patient's access.

As discussed in the **Methods**, no attempt was made to cannulate patient accesses with a third needle during dialysis to measure P_v. For this reason, comparison of prediction and measurement exists for only two of the four parameters in Table 4.

Base case parameters

The parameters listed as "Chosen" in the first column of Table 2 were employed along with "Measured" values for R_b, R_v and L_p and "Predicted" values for P_v and R_d as a "base case" parameter set for simulations (Table 3). Examples of those predictions are shown in Figures 1, 3 and 4.

Comparison of model simulations and patient data

Base case predictions of driving forces on either side of the dialyzer are shown along with the mean ± SD of pressures from Table 1 in the top panel of Figure 1. Individual driving forces, blood pressure (P_b), dialysate pressure (P_d) and plasma oncotic pressure (Π_p), as well as their sum are plotted as a function of position (x/L) along the dialyzer axis. When the sum of these driving forces becomes negative, J_v reverses sign and backfiltration commences.

The model predicts a marked rise in blood side pressure with increasing patient hematocrit. Base case predictions of P_{bi} and P_{bo} are provided along with measurements (Table 1) in the bottom panel of Figure 1. Predictions agree remarkably well with patient data.

The results of individual simulations of 30 dialyses are shown

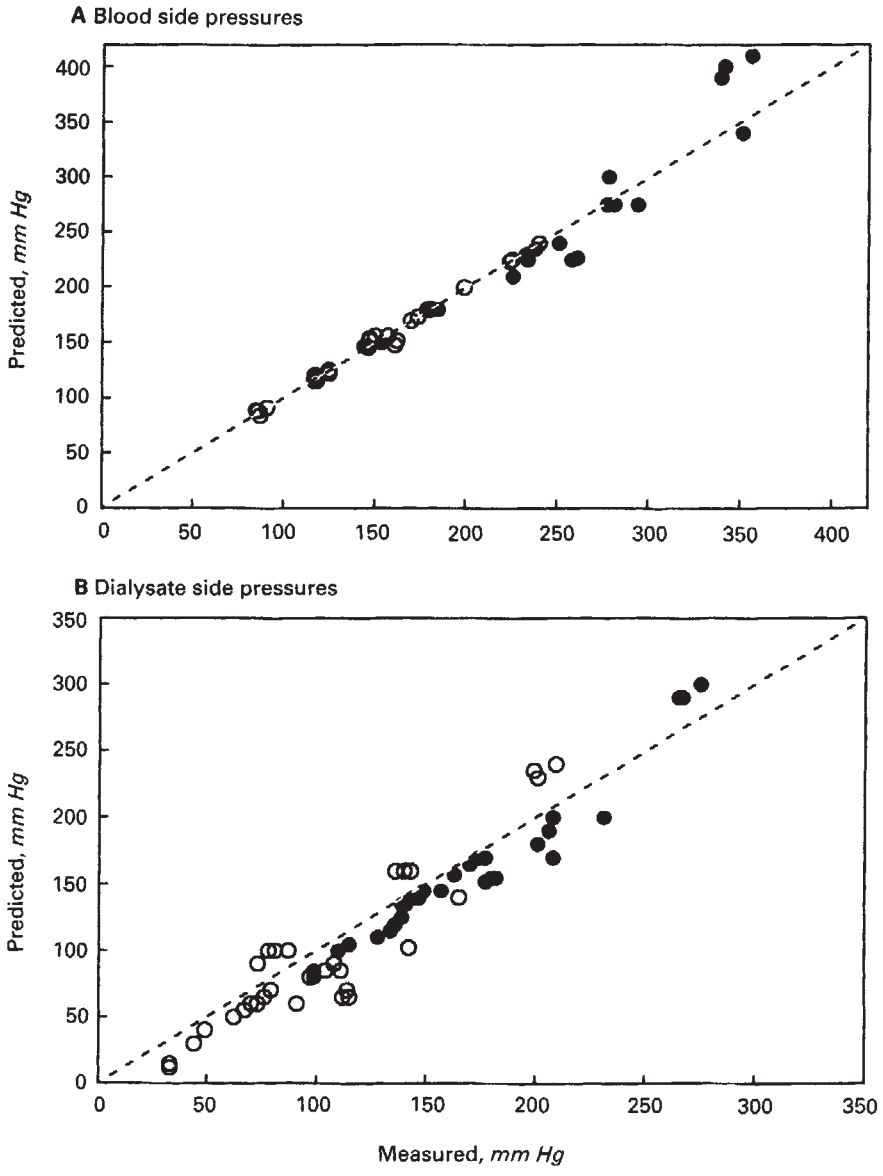

Fig. 2. *Individual patient dialysis.* Dialyzer inlet (filled circles) and outlet pressures (open circles) are shown for the blood (top panel) and dialysate (bottom) sides of the circuit. The dashed line represents identity. Thirty simulations were performed. Many points overlap.

in Figure 2. Predictions of blood side pressures agreed remarkably well with measured values. The model tended to underestimate dialysate side pressures but the error was not large.

Factors which elevate circuit pressure

Perturbations of base case parameters indicate that circuit pressures are most strongly affected by changes in blood flow rate (Q_b), blood access pressure (P_v) and hematocrit (H). The effects of varying the venous pressure at the end of the circuit (P_v) and systemic hematocrit (H) are explored in Figure 3. As shown in the top panel, increasing P_v from 20 to 100 mm Hg results in a parallel rise in blood and dialysate pressures. Net driving forces favoring forward or backfiltration along the dialyzer axis are not altered and the point at which $P_b = P_d$ is constant. Increasing hematocrit from 0.2 to 0.4 also produces a marked increase in circuit pressures (Fig. 3B). In contrast to alterations in P_v, net driving forces at any value of x/L change with increases in H. Also, the point at which $P_b = P_d$ moves closer to the dialyzer entrance and backfiltration begins sooner. The nearly exponential increase of blood viscosity with increasing hematocrit is responsible for this phenomenon.

Effect of filtration rate and hematocrit on backfiltration

The effect of increasing the rate of filtration (Q_f) is explored at hematocrits of 0.2 to 0.4 in Figure 4. In the top panel, the location at which backfiltration commences $(x/L)_{Eq}$ is given as a function of Q_f for the base case inputs. In the bottom panel, the rate of backfiltration (Q_{back}) is provided. Increasing the filtration rate moves the equilibrium point toward the blood exit and reduces the rate of backfiltration. Doubling hematocrit also has a large effect, moving the equilibration point toward the dialyzer entrance and increasing backfiltration. In a patient with a hematocrit of 40% undergoing no net ultrafiltration, equilibrium is reached at the mid point of the dialyzer and backfiltration is predicted to be 1.4 liters/hr.

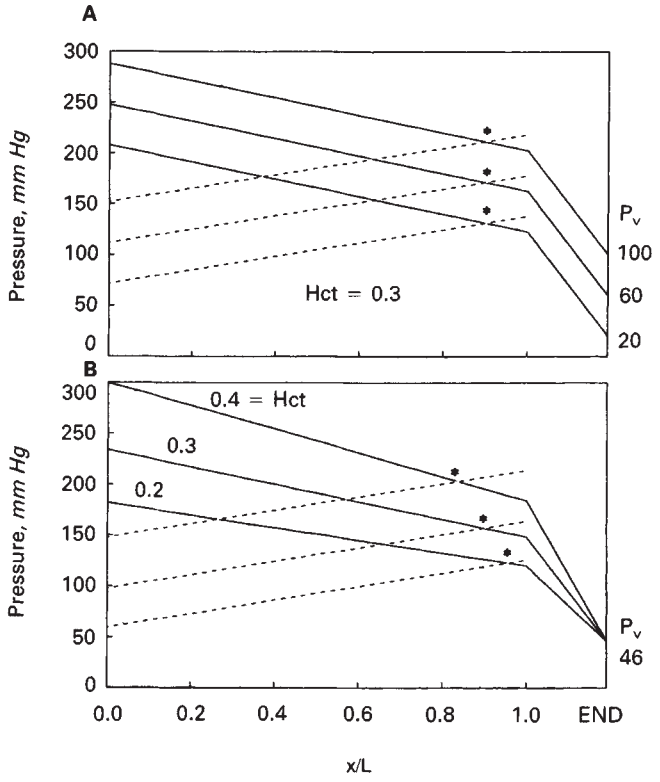

Fig. 3. *Factors which increase circuit pressures.* **A.** Model predictions of blood side (solid lines) and dialysate side (dashed lines) pressures are shown as a function of location (x/L) along the dialyzer axis for access pressures (P_v) of 20 to 100 mm Hg and a systemic hematocrit of 0.30. "*" refers to the point at which blood and dialysate pressures become equal. Solid lines extending from 1.0 to END show the pressure drop from the dialyzer outlet to the patients' access. **B.** Symbol conventions are identical to top panel. Model predictions of blood and dialysate side pressures are shown for three hematocrits at a single access pressure (P_v = 46 mm Hg).

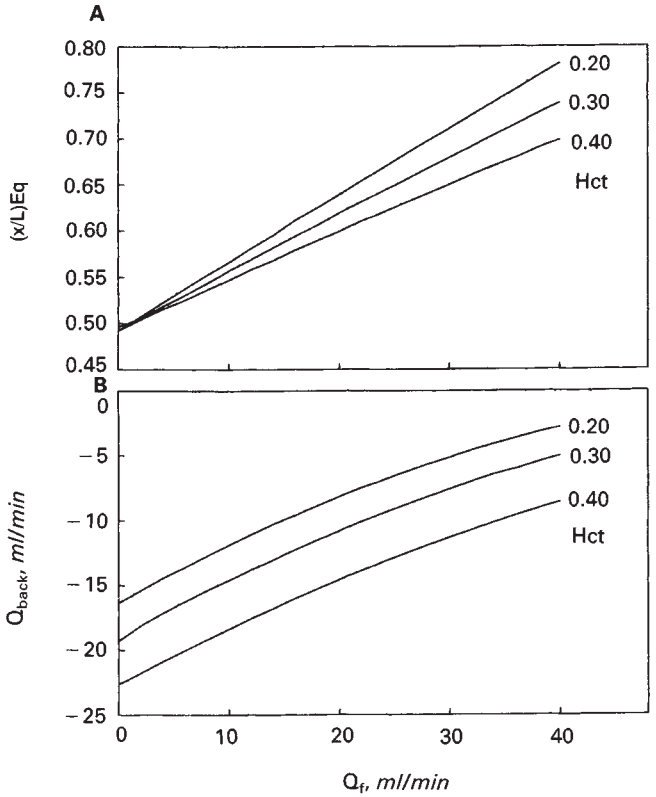

Fig. 4. *Effect of filtration rate and hematocrit on backfiltration.* **A.** The dimensionless location $(x/L)_{Eq}$ at which backfiltration commences is given as a function of filtration rate (Q_f) and three hematocrit levels. Computations otherwise employ base case parameters. **B.** The rate of backfiltration (Q_{back}) is given as a function of filtration rate, Q_f.

Elimination of backfiltration

As an example of the use of this model, computations were performed to estimate the degree to which alteration of critical parameters would influence the rate of backfiltration (Q_{back}, Table 5). Base case values (Table 2) were employed as inputs to yield an estimate of base case backfiltration rate (Q_{back} = 9.3 ml/min, first line Table 5). The parameters listed in the first column were changed from base case values to those listed in the column "Perturbation." The predicted Q_{back} for these perturbations is listed in the last column of Table 5. Increases in blood flow rate, dialyzer length or hydraulic conductivity were predicted to increase Q_{back}. Increases in net filtration rate and hollow fiber radius decreased Q_{back}.

Table 5. Effect of parameter changes on backfiltration

Parameter	Base case value	Perturbation	Q_{back} *ml/min*
Base case	Table 2	None	9.3
Q_b	450	350	6.5
		550	10.8
Q_f	33.3	0.0	21.5
		60.0	2.7
L[a]	22.5	17.5 (N_f = 17,357)	4.5
		27.5 (N_f = 11,045)	14.2
r_f[b]	0.01	0.02 (N_f = 6,750)	0.8
		0.02 (N_f = 13,500)	0.3
L_p	6.91×10^{-5}	3×10^{-5}	−0.5
		9×10^{-5}	14.7

Units employed are given in Table 2 and the Appendix.
[a] Surface area kept constant by altering the number of hollow fibers (N_f)
[b] Surface area either held constant by reducing N_f or allowed to increase by maintaining N_f at 13,500

Discussion

This study describes a model of the hemodialysis circuit which enables prediction of blood and dialysate pressures, as well as the rate of forward and backfiltration during volumetrically-controlled high flux dialysis. The underlying theory is an extension of that employed to describe other extracorporeal circuits [2, 3].

An advantage of the current approach is that the entire blood side of the circuit rather than just the dialyzer is considered. This enables prediction of blood and dialysate side pressures to be obtained from knowledge of circuit component characteristics, patient characteristics (systemic hematocrit and protein concentration), the patient's access pressure and dialyzer hydraulic conductivity. Thus blood and dialysate pressures are predicted rather than required as inputs (Table 3, Mode 2). The

model is flexible and allows an alternative method of computation. If pressure measurements are known, they can be used to obtain estimates of essential parameters that are otherwise difficult to measure. These can subsequently be used to explore model predictions for a particular set of circuit components (Table 3, Mode 1). We have tested the model by measuring both the pressures and the essential parameters. Good agreement was found when the model was used to predict one set of measurements from the other (Table 4, Fig. 1), lending confidence to the theory which underlies the equations.

Other investigators have provided models of the high flux dialyzer [17, 18]. Although they did not consider the entire circuit, many of the same conclusions were reached. The increase in backfiltration rate with rising hematocrit was emphasized by both Stiller, Mann and Brunner [17] and Robertson and Curtin [18]. This study provides both theoretical and in vivo data to corroborate that prediction.

The model is defined by simple ordinary differential equations using one of two interaction schemes. In practice, convergence is obtained in 10 to 30 seconds on an IBM compatible microcomputer. This permits the model to be explored in a short time while parameters are varied over a large range. We conclude that radial variations of protein and RBC concentrations within the dialyzer can be neglected (see below) so that the need to solve time consuming finite difference equations is avoided [18].

Elevated circuit pressures

Schwab and colleagues have pointed out the importance of monitoring elevated circuit pressures as a sentinel of venous stenosis and incipient access thrombosis [19]. Windus et al demonstrated that a well-functioning access is essential for the patient to obtain the benefits of high-efficiency dialysis [20]. The model predicts that increases in access pressure will be reflected by an equivalent pressure increase on the blood and dialysate sides of the high-flux hemodialysis circuit. With regard to the quality of blood access, this model can provide a method of analysis by permitting hematocrit and plasma protein concentration to be dissected out as separate variables that contribute to elevations of blood side pressures. A patient with a low hematocrit and high access pressure might show as high a blood side outlet pressure as one with a high hematocrit and low access pressure (Fig. 2), suggesting possible utilization of this model to avoid unnecessary fistulograms.

Backfiltration

With highly permeable membranes, it is possible for several liters of dialysate to be transported across the dialyzer membrane into the blood during each dialysis treatment (Fig. 4, Table 5). New membrane materials (for example, polysulfone) do not reject solutes of intermediate molecular weight, raising concern about exposure of patients to bacterial endotoxins. An extensive review of this issue, its prevalence and strategies to eliminate it has been provided by Ronco [21]. The current model corroborates many features of that description. The backfiltration phenomenon was recently investigated in an in vitro study by Leypoldt, Schmidt and Gurland [22]. Dialysate containing an impermeant macromolecule was obtained from locations along the dialyzer axis by sampling from ports placed in the jacket. Dilution and concentration of the marker was observed providing verification of the existence of backfiltration. Those authors found that in dialyzers with intermediate ultrafiltration coefficients (hydraulic conductivity), backfiltration was readily eliminated by low rates of net ultrafiltration. In the presence of a highly permeable membrane material (polysulfone), however, backfiltration was not readily eliminated. Our findings are in agreement. Current simulations and data focus on a polysulfone dialyzer with a very high hydraulic conductivity. As shown in Table 5, elimination of backfiltration is predicted to be most readily accomplished by reducing hydraulic conductivity. In contrast, increasing ultrafiltration rate to 3.6 liters/hr may fail to accomplish this task. As discussed by Ronco, the perturbations in Table 5 do not represent an exhaustive list of strategies that may effectively reduce or eliminate backfiltration [21].

Model limitations

Dialysate side resistance to flow. In this study, the dialysate side of the dialyzer has been treated as a simple resistance to flow (equation 4). No theory, such as the Hagen-Poiseuille equation for laminar flow in a tube, supports this approach. Due to the low viscosity of dialysate and its high velocity, the Reynolds number is expected to be high so that turbulent rather than laminar flow probably exists [5, 6]. The current success in simulating patient data undoubtedly arises from the fact that the inlet dialysate flow rate was always equal to 800 ml/min. The small alteration in flow rate resulting from the addition of filtrate at 20 to 30 ml/min is expected to produce little change in the decline of dialysate side pressure from patient to patient. This has two consequences. First, as Stiller et al assumed [17], the predicted dialysate pressure profile is virtually linear because Q_d (equation 6) is nearly constant. It is therefore not surprising that a single value for R_d yields reasonable predictions of dialysate pressures (Fig. 1). Second, it is theoretically unsound to extrapolate the use of R_d obtained at 800 ml/min to another dialysate flow rate.

Concentration polarization. As proteins are rejected at the membrane surface they must diffuse back toward the center of the fibers at the same rate. This process must, to some degree, result in the establishment of a radial protein concentration gradient (concentration polarization) [23]. If this gradient is large, calculation of membrane fluxes on the basis of Starling forces and bulk protein concentration will give incorrect results. We [2] and Lysaght, Schmidt and Garland [24] concluded that such boundary layer effects during continuous arteriovenous hemofiltration (CAVH) appear to be minimal. During high flux dialysis filtration can be as high as 30 ml/min, a rate which is higher than that reached during CAVH (7 to 12 ml/min). Nonetheless, during high flux, a lower average radial fluid velocity perpendicular to the membrane exists because surface area for filtration (Fresenius F80, 1.8 m^2) is at least five times larger (Amicon Diafilter-20, 0.25 m^2). Thus, neglect of concentration polarization is even more justified in the current setting. Furthermore, the agreement we find between measured and predicted hydraulic conductivity (L_p, Table 4) is good, providing experimental evidence that concentration polarization of protein can be neglected. It must be recognized, however, that neglect of concentration polarization prohibits extrapolation of this model to conditions that involve maximal filtration rates with fluid replacement (hemodiafiltration) [25].

Blood rheology. Formulation of this model neglects the partitioning of blood and plasma within hollow fibers of the dialyzer that may alter apparent viscosity and hematocrit. The

rationale for this is identical to that previously described for 200 micron diameter fibers [2, 26]. Like previous models, it follows that extrapolation to small diameter hollow fiber geometry is not permissible without reformulation to account for the Fahraeus and Fahraeus-Lindqvist effects [12, 13].

Summary

We have provided a mathematical model that simulates the hemodynamics on the blood side and dialysate sides of the high-flux hemodialysis circuit. The model accepts patient and circuit characteristics as inputs and returns predictions of hydraulic and oncotic pressure distribution, hematocrit and blood viscosity, location and degree of forward and backfiltration. The model successfully reproduces data obtained from patient dialyses with the Fresenius F80 dialyzer. Increased patient access pressure is predicted to produce a parallel rise in blood and dialysate circuit pressures without affecting the location or extent of backfiltration. In contrast, increases in hematocrit and blood viscosity are expected to increase circuit pressures while enhancing the rate of backfiltration. Possible uses include evaluation of the quality of patient blood accesses, optimization of dialyzer design and choice of dialysis circuit components.

Reprint requests to Thomas L. Pallone, M.D., Division of Nephrology, M.S. Hershey Medical Center, Hershey, Pennsylvania 17033, USA.

Appendix. Abbreviations

Symbols and units

C	concentration (g/dl)
H	systemic hematocrit
J_v	transmembrane volume flux (cm/min)
L_p	hydraulic permeability [cm/(min · mm Hg)]
L	dialyzer length (cm)
N_f	the number of hollow fibers
P	pressure (mm Hg)
Q	flow rate (ml/min)
R	resistance ($1/cm^3$)
S	membrane surface area (cm^2)
T	temperature (°C)
x	axial position along the dialyzer (cm)

Greek letters

ϕ	local hematocrit
μ	viscosity (mm Hg · min)
Π	oncotic pressure (mm Hg)

Subscripts

b	blood
c	cellular compartment, red blood cells
d	dialysate
f	filtrate
i	inlet
o	outlet
p	plasma
v, vn, vt	venous, venous needle, venous tubing
w	water
20, 37	value at 20°C or 37°C

Superscripts

′	normal value for human blood

References

1. Collins AH, Keshaviah PR: Are there limitations to shortening dialysis treatment? *Trans ASAIO* 34:1–5, 1988
2. Pallone TL, Petersen J: Continuous arteriovenous hemofiltration: An in vitro simulation and mathematical model. *Kidney Int* 33:685–698, 1988
3. Pallone TL, Hyver SW, Petersen J: The simulation of continuous arteriovenous hemodialysis with a mathematical model. *Kidney Int* 35:125–133, 1989
4. Lowry OH, Rosenbrough NJ, Farr AL: Protein measurement with the folin phenol reagent. *J Biol Chem* 193:265–275, 1951
5. Sabersky RH, Acosta AJ, Hauptman EG: *Fluid Flow* (2nd ed), New York, MacMillan Publishing Co., Inc., 1971, p. 222
6. Colton CK, Smith KA, Strove P, Merrill EW: Laminar flow mass transfer in a flat duct with permeable walls. *A I ChE J* 17:773–780, 1971
7. Starling EH: On the absorption of fluids from connective tissue spaces. *J Physiol* 19:312–326, 1896
8. Landis EM, Pappenheimer JR: Exchange of substances through the capillary wall, in *Handbook of Physiology. Circulation.*, Washington, D.C., Am. Physiol. Soc., 1963 (sect 2, vol. II, chapt. 29), pp. 962–1034
9. Merrill EW: Rheology of blood. *Physiol Rev* 49:863–888, 1969
10. Merrill EW, Gilliland ER, Cokelet G, Shin H, Britten A, Wells RE: Rheology of human blood near and at zero flow. Effects of temperature and hematocrit level. *Biophys J* 3:199–213, 1963
11. Vand V: Viscosity of solutions and suspensions. Part I. J. *Phys Colloid Chem* 52:300–305, 1948
12. Fahraeus R: The suspension stability of blood. *Physiol Rev* 9:241–274, 1929
13. Fahraeus R, Lindqvist T: The viscosity of the blood in narrow capillary tubes. *Am J Physiol* 96:562–568, 1931
14. Dintenfass L: *Blood Viscosity, Hyperviscosity, and Hyperviscosaemia.* Boston, MTP Press Limited, 1985, pp. 19–21
15. *Handbook of Chemistry and Physics* (51st ed), Edited by Weast RC, 1970-71, p. F36
16. Gear CW: *Numerical Initial Value Problems in Ordinary Differential Equations.* Englewood Cliffs, Prentice-Hall, 1971
17. Stiller S, Mann H, Brunner H: Backfiltration in hemodialysis with highly permeable membranes. *Contr Nephrol* 46:23–32, 1985
18. Robertson BC, Curtin C: Effects of EPO therapy on backfiltration in high flux dialysis. *Trans ASAIO* 36:447–452, 1990
19. Schwab SJ, Raymond JR, Saeed M, Newman GE, Dennis PA, Bollinger RR: Prevention of hemodialysis fistula thrombosis. Early detection of venous stenosis. *Kidney Int* 36:707–711, 1989
20. Windus DW, Audrain J, Vanderson R, Jendrisak MD, Picus D, Delmez JA: Optimization of high-efficiency hemodialysis by detection and correction of fistula dysfunction. *Kidney Int* 38:337–341, 1990
21. Ronco C: Backfiltration in clinical dialysis: Nature of the phenomenon, mechanisms and possible solutions. *Int J Artif Organs* 13:11–21, 1990
22. Leypoldt JK, Schmidt B, Gurland HJ: Net ultrafiltration may not eliminate backfiltration during hemodialysis with highly permeable membranes. *Artif Organs* 15:164–170, 1991
23. Reihnian H, Robertson CR, Michaels AS: Mechanisms of polarization and fouling of ultrafiltration membranes by proteins. *J Membrane Sci* 16:237–258, 1983
24. Lysaght MJ, Schmidt B, Garland HJ: Filtration rates and pressure driving force in AV filtration. *Blood Purif* 1:178–183, 1983
25. Colton CK, Henderson LW, Ford CA, Lysaght MJ: Kinetics of hemodiafiltration. I. In vitro transport characteristics of a hollow-fiber blood ultrafilter. *J Lab Clin Invest* 85:355–371, 1975
26. Gaehtgens P: Flow of blood through narrow capillaries: Rheological mechanisms determining capillary hematocrit and apparent viscosity. *Biorheology* 17:183–189, 1980